

# FIELD DATA FROM A CAPILLARY BARRIER AND MODEL PREDICTIONS WITH UNSAT-H

By Milind V. Khire,<sup>1</sup> Craig H. Benson,<sup>2</sup> and Peter J. Bosscher,<sup>3</sup> Members, ASCE

**ABSTRACT:** Water balance data are presented from a capillary barrier test section located on the final cover of a municipal solid waste landfill in a semiarid region (E. Wenatchee, Washington, U.S.). Water balance and meteorological data were collected from November 1992 to August 1995. Estimates of the water balance were made using the program UNSAT-H, with input consisting of meteorological data, soil properties, and vegetative information. Estimates of evapotranspiration and soil-water storage by UNSAT-H agree reasonably well with the field data. Peak soil-water storage was underestimated during the winter and evapotranspiration was overestimated in late winter. Water contents were estimated reasonably, although the changes in water content of the sand obtained from UNSAT-H were not as large as, and occurred less quickly than, that in the field. Percolation was generally overestimated, with the greatest overestimation occurring during Winter 1993, which had substantial snowfall. Surface runoff was underestimated; no runoff was obtained from UNSAT-H, whereas 7.4 cm of runoff was measured in the field. The overestimates in percolation appear to be closely related to underestimates in runoff and extra storage in the sand layer caused by the geocomposite drain used in the test section. Snowmelt, freezing of the soil surface, and hysteresis in soil hydraulic properties also appear to have had an effect on the differences between estimated and measured water balances.

## INTRODUCTION

Arid and semiarid regions are often considered ideal locations for waste disposal. Research has shown, however, that recharge comprising as much as 50% of precipitation can occur in these regions (Gee and Hillel 1988; Nativ 1991; Gee et al. 1992, 1994; Allison et al. 1994; Fayer et al. 1996), which can result in ground-water contamination from uncontained waste disposal facilities. Research has also shown that earthen covers that store precipitation and then release it back to the atmosphere can be effective and economical barriers to percolation in semiarid and arid environments (Nyhan et al. 1990; Gee et al. 1993; Ward and Gee 1997; Morris and Stormont 1997; Dwyer 1997). One type of earthen cover is a capillary barrier, which is defined here as a cover employing a finer-grained layer overlying a coarser-grained layer. This contrast in particle size limits downward migration of water by exploiting the contrasting unsaturated hydraulic properties of soils with different gradation. Capillary barriers are practical for semiarid and arid regions because there is no need for moisture conditioning, which reduces construction costs. In addition, because capillary barriers do not have a moist, compacted clay layer, they are less susceptible to degradation caused by desiccation cracking.

A model that simulates water balance with reasonable accuracy is a necessary tool for hydrologic design of earthen covers incorporating capillary barriers. For semiarid and arid regions, the model must be fairly sophisticated because of the complex interactions between precipitation, evapotranspiration, and unsaturated flow that occur in such regions (Fleener and King 1995; Khire et al. 1997). One model designed especially for this application is Unsaturated Water and Heat Flow (UNSAT-H) (Fayer and Jones 1990), which was developed at Pacific Northwest Laboratory in Richland, Washing-

ton, to evaluate recharge and cover designs at the Hanford Site. UNSAT-H employs a one-dimensional finite-difference solution of Richards' equation, and contains a constitutive approach for managing water at the soil-atmosphere boundary. Fayer et al. (1992) show that UNSAT-H predicted fairly accurately the water balance of several small test lysimeters containing capillary barriers. Khire et al. (1997) also report a favorable comparison between field-measured water balances and estimates by UNSAT-H for two large resistive barrier test sections (i.e., final covers where barrier layers having low saturated hydraulic conductivity provide the primary resistance to flow), constructed in humid and semiarid climates.

In this paper a comparison is made for a capillary barrier test section constructed in a semiarid climate. The water balance of the test section is described, along with water balance estimates made with UNSAT-H. The common HELP model (Schroeder et al. 1994) was not used because HELP does not contain algorithms to simulate unsaturated flow rigorously (Nichols 1991), which can result in gross errors when simulating capillary breaks (Benson et al. 1993). In another publication (Khire et al. 1998), UNSAT-H is used to examine how design variables affect the performance of capillary barriers.

## CAPILLARY BARRIERS

Recent field studies have suggested that capillary barriers can be used for restricting percolation in semiarid and arid climates (Gee et al. 1993; Nyhan et al. 1993; Hakonson et al. 1994; Stormont 1995; Gee and Ward 1997; Nyhan et al. 1997). Capillary barriers are constructed in various forms, ranging from a simple design consisting of two layers to more complex designs that include multiple layers of finer-grained and coarser-grained soils (e.g., Stormont 1995; Morris and Stormont 1997; Stormont and Morris 1997; Nyhan et al. 1997). In its basic form, however, a capillary barrier consists of a finer-grained layer overlying a coarser-grained layer [Fig. 1(a)] (Benson and Khire 1995). The contrast in particle size limits downward migration of water by (1) storing water in the upper finer-grained layer until it can be later removed by evaporation and transpiration, or (2) diverting the water laterally in the surface layer (e.g., Hakonson et al. 1994; Stormont 1995). When the annual precipitation is low (e.g., <30 cm) and the finer-grained layer is silty or clayey, storage in the finer-grained layer and subsequent evapotranspiration is often con-

<sup>1</sup>Asst. Proj. Engr., GeoSyntec Consultants, Boca Raton, FL 33487. E-mail: Miles@GeoSyntec.com

<sup>2</sup>Assoc. Prof., Dept. of Civ. and Envir. Engrg., Univ. of Wisconsin, Madison, WI 53706. E-mail: chbenson@facstaff.wisc.edu

<sup>3</sup>Assoc. Prof., Dept. of Civ. and Envir. Engrg., Univ. of Wisconsin, Madison, WI. E-mail: bosscher@enr.wisc.edu

Note. Discussion open until November 1, 1999. To extend the closing date one month, a written request must be filed with the ASCE Manager of Journals. The manuscript for this paper was submitted for review and possible publication on September 2, 1997. This paper is part of the *Journal of Geotechnical and Geoenvironmental Engineering*, Vol. 125, No. 6, June, 1999. ©ASCE, ISSN 1090-0241/99/0006-0518-0527/\$8.00 + \$.50 per page. Paper No. 16538.

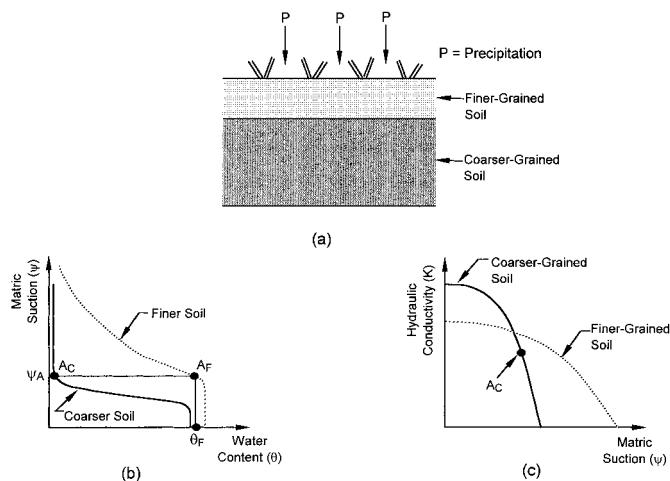


FIG. 1. Schematics of Capillary Barrier (a); Unsaturated Hydraulic Conductivity Functions (b); and Soil-Water Characteristic Curves (c) for Finer- and Coarser-Grained Soils

sidered the primary means of preventing downward movement of water (Meyer et al. 1996).

A capillary barrier limits downward migration of water because the finer-grained surface layer must become nearly saturated before water will enter the coarser-grained soil. Water will enter the coarser soil when the matric suction at the surface of the coarser layer decreases to the value corresponding to the rapid change in slope near residual water content in the soil-water characteristic curve (Stormont and Anderson 1998). This point is noted as  $A_c$  in Fig. 1(b), and the corresponding matric suction is  $\psi_A$ . Since continuity in pore-water pressure requires that the matric suction be equal at the interface between the two layers, the matric suction in the finer layer at the interface must equal  $\psi_A$  before water will enter the coarser layer. This water content is noted as  $\theta_F$  in Fig. 1(b);  $\theta_F$  is near saturation and corresponds to point  $A_f$  on the soil-water characteristic curve for the finer layer. Even when  $A_f$  is reached, water still enters the coarser-grained layer slowly because the hydraulic conductivity of the coarser-grained layer is still low at  $A_c$  [Fig. 1(c)], and is generally lower than that of the finer-grained layer.

Design of capillary barriers requires a water balance model that reasonably simulates unsaturated flow, and surface energy and water balances. Evaluating water balance programs suitable for capillary barriers was one of the key objectives of this study. As with other covers, a capillary barrier is susceptible to degradation by erosion and biota intrusion (Khire et al. 1994; Litgotke 1994; Landeen 1994; Hakonson et al. 1992; Benson and Khire 1995). These factors are not considered in this paper but are an important aspect of capillary barrier design.

## FINAL COVER TEST SECTION

The capillary barrier test section was constructed on the final cover at the Greater Wenatchee Regional Landfill in East Wenatchee, Washington. East Wenatchee is in central Washington State, 236 km east of Seattle and 110 km north of the Hanford site (Hanford, Wash.). The average annual precipitation in East Wenatchee is 23 cm. Most of the precipitation occurs in late fall and winter in the form of rain or snow. Snowfall typically comprises 30% of annual precipitation (Khire et al. 1994). East Wenatchee is slightly wetter and receives more snowfall than the Hanford site (Ward and Gee 1997), and is categorized as a cool desert (Link et al. 1995).

The test section is 30 × 30 m areally, of which a 18.3 × 12.2 m region is used for monitoring. The surface layer is 15 cm of uncompacted, sparsely vegetated sandy silt (SM-ML)

and the underlying layer is 75 cm of clean, uniformly graded medium sand (SP). Index properties of these soils are reported in Benson et al. (1994). Both soils were obtained on-site. A thicker surface layer would be used in practice to ensure that it would have sufficient storage capacity to handle a broad variety of meteorological events that could occur during the design life of the cover, while maintaining acceptable percolation. For example, at the Wenatchee site the surface layer needs to be at least 60 cm thick to maintain percolation below that for the prescribed resistive cover (Benson et al. 1998). At the Hanford site, a surface layer 2 m thick was required to reduce percolation to less than 0.5 mm/yr (Gee and Ward 1997). However, the objective of this study was to determine if the capillary barrier effect and the water balance of the cover could be modeled. Thus, a thin surface layer was used to ensure that water would penetrate the coarser layer and measurable percolation would occur. Had a much thicker surface layer been used, flow into the coarser layer may not have occurred and no percolation may have been transmitted.

Selection of an appropriate surface layer thickness is beyond the scope of this paper but is an important issue affecting long-term performance of alternative earthen covers. Details regarding how to determine the appropriate surface layer thickness can be found in Stormont and Morris (1998), Stormont and Anderson (1998), and Khire et al. (1998).

The test section is instrumented for continuous monitoring of climatic data, runoff, soil-water content, and percolation. Runoff is collected via diversion berms (Fig. 2). Time domain reflectometry (TDR) is used to measure soil-water content, and soil-water storage is computed by integrating soil-water contents over the depth of the test section (Ward and Gee 1997). Benson et al. (1994) provide a detailed description of how the test section was constructed and instrumented.

Percolation is collected using a lysimeter 12.2 m wide × 18.3 m long (Fig. 2), constructed from high density polyethylene (HDPE) geomembrane and a geocomposite drain. The geocomposite drain also forms a capillary barrier that causes water to be stored in the sand, that would not be stored if the sand layer were deep (e.g., >3 m). Thus the test section is representative of a cover placed directly on porous waste or on a coarse biota barrier used to prevent intrusion into underlying waste. A deeper lysimeter could have been used to simulate the condition where a coarse underlying layer is not present, but this option was not possible within the economic and regulatory constraints of the project. Moreover, recent data describing the unsaturated hydraulic properties of municipal solid waste (MSW) suggest that the air and water entry pressures for solid waste are very low (~1 to 2 cm, Benson and Wang 1998). Thus, the capillary barrier effect afforded by the geocomposite drain probably would be manifested by a cover placed on MSW.

Evapotranspiration ( $E_t$ ) is computed by subtracting daily runoff ( $R$ ), percolation ( $P_r$ ), lateral flow ( $L_r$ ), and the change in the soil-water storage ( $\Delta S$ ) from daily precipitation ( $P$ ), as shown in the following equation (Tanner 1967):

$$E_t = P - R - P_r - L_r - \Delta S \quad (1)$$

Lateral flow ( $L_r$ ) is assumed to be zero in this study. Khire

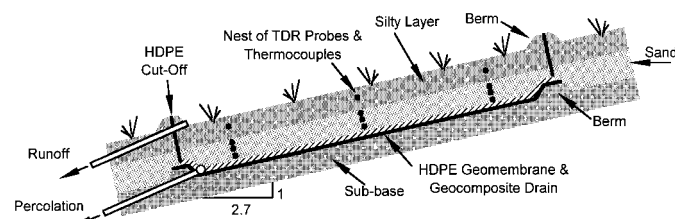


FIG. 2. Cross Section of Instrumented Test Section

(1995) indicates that lateral flow was less than 0.01% of total precipitation, suggesting that ignoring lateral flow is reasonable. Evapotranspiration computed using (1) is a residual quantity and thus includes random and systematic measurement errors.

## SOIL HYDRAULIC PROPERTIES

### Soil-Water Characteristic Curves

Undisturbed specimens from the silty surface layer were trimmed from block specimens (diameter = 200 mm) obtained from the test sections for measuring moisture-retention properties. Specimens of the sand were prepared in the laboratory to the average gravimetric water content and compacted to the average dry unit weight measured during construction. Details of the sampling and preparation methods can be found in Khire et al. (1994) and Benson et al. (1993, 1994). The soil-

water characteristic curve for the silty layer was measured in a pressure-plate extractor, in which a maximum pressure of 415 kPa was applied. A hanging column equipped with a Buchner funnel was used for the sand. Only desorption curves were measured.

Soil-water characteristic curves (SWCCs) for the soils are shown in Fig. 3. The graphs include measurements made in the laboratory, as well as checks in the field that were made using tensiometers installed in the test section. The tensiometer data (marked by open squares in Fig. 3) agree reasonably well with the data from the laboratory tests (marked by open circles). Fits of the Haverkamp function (Haverkamp et al. 1977) to the soil-water characteristic curves are also shown. The Haverkamp function has the form

$$\frac{\theta - \theta_r}{\theta_s - \theta_r} = \frac{\alpha}{\alpha + \psi^\beta} \quad (2)$$

where  $\theta$  = water content at matric suction  $\psi$ ;  $\theta_s$  = water content at saturation;  $\theta_r$  = residual water content; and  $\alpha$  and  $\beta$  = Haverkamp fitting parameters. The model fits the data reasonably well, as evinced by the  $R^2 = 0.92$  (silty surface layer) and 0.98 (sand) that were obtained. The Haverkamp function was selected arbitrarily, but it fits the data well and is readily used in UNSAT-H. Moreover, use of the Haverkamp functions permitted independent functions to be fit to the SWCC and the unsaturated hydraulic conductivity data, which was not possible for the other functions that can be used in UNSAT-H.

When fitting (2), the lowest water content measured in the field using TDR (data point marked TDR) was assumed to be the water content corresponding to the wilting point [ $\psi = 15.4$  m (1540 kPa)]. This assumption was not verified, but the reasonable correspondence of the tensiometer data suggests that the assumption is not grossly incorrect. Haverkamp fitting parameters for the cover soils are listed in Table 1.

The soil-water characteristic curve for the silty layer exhibits a more gradual decrease in water content with increasing matric suction [Fig. 3(a)], which is typical for finer-grained soils (Hillel 1980). In contrast, the water content of sand decreases rapidly at small matric suctions [Fig. 3(b)] due to drainage of large pores. At a matric suction of 2 m, the finer-grained silty surface layer is close to saturation ( $\theta \sim 0.3$ ), whereas the sand is almost dry ( $\theta \sim 0.02$ ) (Fig. 3).

### Saturated Hydraulic Conductivity

Saturated hydraulic conductivity of the silty surface layer was measured on three undisturbed block specimens having a diameter of 15 cm and height of 20 cm. The tests were performed in flexible-wall permeameters, following procedures described in ASTM D 5084, using a hydraulic gradient of five and an effective stress of 10 kPa. No backpressure was used. Three specimens of the sand were tested in rigid-wall per-

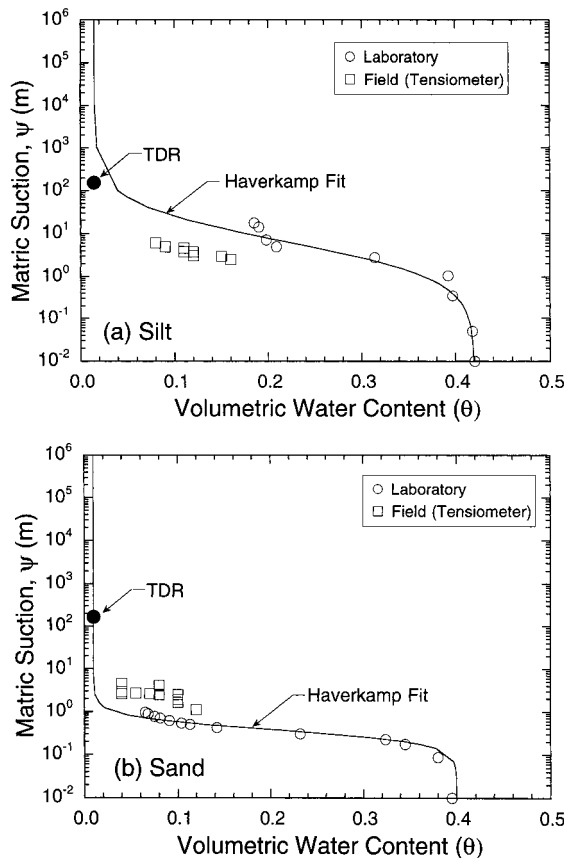


FIG. 3. Soil-Water Characteristic Curves: (a) Silty Layer; (b) Sand

TABLE 1. Soil Properties Input to UNSAT-H

Parameter (1)	Layer (2)	Value (3)	Source (4)
Porosity	Silt surface layer	0.42	Field density test (Lane et al. 1992)
	Sand layer	0.40	
Saturated hydraulic conductivity (m/s)	Silt surface layer	$2.7 \times 10^{-6}$	Laboratory hydraulic conductivity tests (Benson et al. 1993)
	Sand layer	$2.9 \times 10^{-5}$	
Parameters for soil water characteristic curves	Silt surface layer	$\alpha = 650$ , $\beta$ (1/cm) = 100 $\theta_r = 0.015$	Khire et al. (1995)
	Sand layer	$\alpha = 35,000$ , $\beta$ (1/cm) = 290 $\theta_r = 0.01$	
Parameters for unsaturated hydraulic conductivity function	Silt surface layer	$A = 90$ , $B$ (1/m) = 215	Khire et al. (1995)
	Sand layer	$A = 105$ , $B$ (1/m) = 290	
Layer thickness (m)	Silt surface layer	0.15	Measured (Benson et al. 1994)
	Sand layer	0.75	

meameters using a constant head applied with a Mariotte bottle. Procedures described in ASTM D 2434 were followed using a hydraulic gradient of five. The specimens were prepared in the permeameter to the average dry unit weight measured during construction (15.6 kN/m<sup>3</sup>). The geometric mean saturated hydraulic conductivities are reported in Table 1. More details regarding the sampling methods and testing procedures can be found in Benson et al. (1993) and Khire et al. (1994).

### Unsaturated Hydraulic Conductivities

The unsaturated hydraulic conductivity function for the silty surface layer was measured in the laboratory using the instantaneous profile method via evaporation (Benson and Gribb 1997) on a block specimen removed from the test section. The experimental setup was similar to that used by Meerdink et al. (1996). Water contents were measured using TDR probes inserted at five equidistant locations along the length of the specimen (vertical spacing = 3.3 cm). Matric suctions at these points were obtained from the desorption soil-water characteristic curve [Fig. 3(a)] using water contents measured with TDR.

The unsaturated hydraulic conductivity function for the surface layer is shown in Fig. 4(a). The Haverkamp function fit to the unsaturated hydraulic conductivity data is also shown. The Haverkamp function has the following form (Haverkamp et al. 1977):

$$K_{\psi} = K_s \left( \frac{A}{A + \psi^B} \right) \quad (3)$$

where  $A$  and  $B$  = fitting parameters, and  $K_s$  = saturated hydraulic conductivity. Haverkamp fitting parameters for the silty surface layer and sand are listed in Table 1. In this case, the field saturated hydraulic conductivity (i.e., saturated hydraulic conductivity measured without backpressure) was used to simulate the nearly but not completely saturated field condition.

The unsaturated hydraulic conductivity function for the sand was measured in the laboratory and field using the instantane-

ous profile method. Khire et al. (1994) provide a detailed explanation regarding how the measurements were made. The laboratory test was conducted by saturating a specimen of sand (dry unit weight = 15.6 kN/m<sup>3</sup>, 10 cm in diameter, 21 cm in height) and then allowing it to drain under gravity from the bottom. TDR probes inserted into the specimen at six depths were used to measure water contents as the sand drained. Water contents measured with respect to depth and time were used in conjunction with the soil-water characteristic curve [Fig. 3(b)] to calculate unsaturated hydraulic conductivities. Field unsaturated hydraulic conductivities were measured using the procedure described in Meerdink et al. (1996).

Unsaturated hydraulic conductivities of the sand are shown in Fig. 4(b). The Haverkamp model provides a good fit to the sand data ( $R^2 = 0.91$ ) as well as the silty surface layer data ( $R^2 = 0.93$ ). Comparison of the relative hydraulic conductivity functions in Figs. 4(a and b) shows that the hydraulic conductivity of the sand is lower than the hydraulic conductivity of the silty surface layer for matric suctions exceeding approximately 1 m.

### WATER BALANCE MODELING

A water balance model for a capillary barrier in a semiarid climate should possess many attributes, including constitutive algorithms for surface fluxes, a constitutive method for handling runoff, an algorithm to handle temporal and depth-dependent water uptake by plant roots, an ability to account for vapor flow and hysteresis in soil hydraulic properties, and multidimensional flow that accounts for suction-dependent anisotropy. None of the existing models possess all of these attributes. In addition, the multidimensional models that are available do not account for suction-dependent anisotropy or vapor flow, and some have serious computational problems when simulating flow in soils having sharp contrasts in hydraulic properties (e.g., as in capillary barriers). The computational problems are particularly severe when water is applied to the surface sporadically, as occurs under the meteorological conditions in semiarid climates. For these reasons, the one-dimensional model UNSAT-H (ver. 2.0) was selected; it included many of the desired attributes that are believed to have a critical impact on the water balance of capillary barriers (i.e., surface fluxes, runoff, vapor flow, temporal and depth-dependent root water uptake). The model was also computationally stable for the conditions being simulated.

UNSAT-H is a finite-difference computer program for simulating water and heat flow in earthen covers. It solves Richards' partial differential equation for liquid water flow modified for vapor flow and root uptake, and Fourier's equation for heat flow. Only isothermal water flow was considered in this study. Meyer et al. (1996) report that similar results are obtained when isothermal conditions are assumed, and that simulating nonisothermal conditions increases CPU times by a factor of about 60. The form of Richards' equation solved by UNSAT-H is

$$\frac{\partial \theta}{\partial \psi} \frac{\partial \psi}{\partial t} = - \frac{\partial}{\partial z} \left[ K_T \frac{\partial \psi}{\partial z} + K_{\psi} + q_{VT} \right] - S(z, t) \quad (4)$$

where  $\psi$  = matric suction;  $t$  = time;  $z$  = vertical coordinate;  $K_{\psi}$  = unsaturated hydraulic conductivity;  $K_T = K_{\psi} + K_{V\psi}$ , where  $K_{V\psi}$  is isothermal water vapor conductivity (Fayer and Gee 1992);  $q_{VT}$  = thermal vapor flux density; and  $S(z, t)$  is a sink term representing water uptake by vegetation. The thermal vapor flux density ( $q_{VT}$ ) is computed using Fick's law of vapor diffusion. Hysteresis in the soil-water characteristic curve is not considered. Details regarding the algorithm can be found in Fayer and Jones (1990). UNSAT-H was used to conduct water balance simulations of the capillary barrier test section for the period between November 1992 and May 1995.

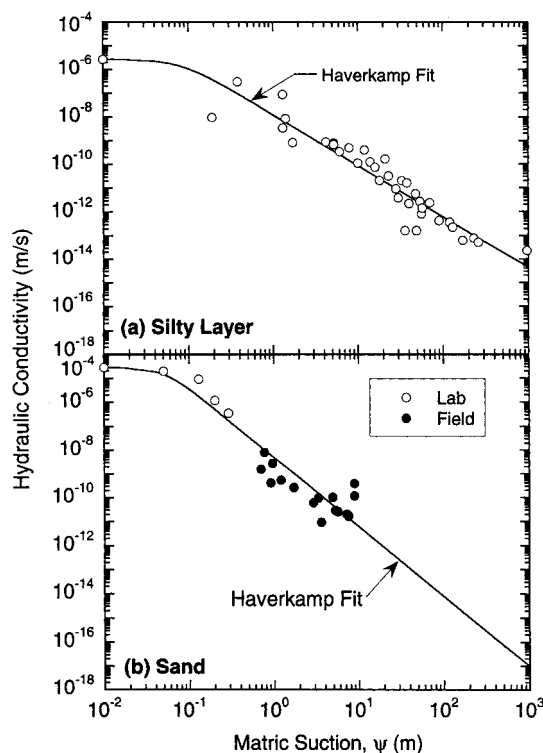


FIG. 4. Unsaturated Hydraulic Conductivity Functions: (a) Silty Layer; (b) Sand

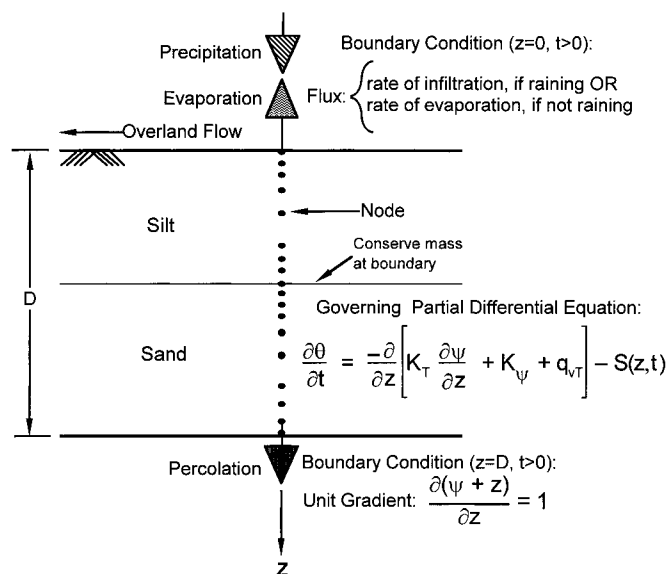


FIG. 5. Conceptual Model for UNSAT-H

A schematic showing how UNSAT-H computes the water balance components is shown in Fig. 5. UNSAT-H is a one-dimensional model and thus does not compute lateral drainage. UNSAT-H separates precipitation falling on a cover into infiltration and runoff. The quantity that infiltrates depends on the infiltration capacity of the soil profile immediately prior to rainfall (e.g., Khire et al. 1997). If precipitation during a time-step exceeds the infiltration capacity, the extra water is shed as runoff, which prevents ponding from occurring. UNSAT-H does not consider absorption and interception of water by the plant canopy or delayed infiltration of runoff when computing runoff. Despite these limitations, Khire et al. (1997) report that UNSAT-H can simulate runoff as well as conventional runoff models.

Water that infiltrates moves upward due to evaporation, or downward as a consequence of gravity and matric potential (Fig. 5). When the upper boundary is a flux boundary, infiltration and evaporation from the surface can be used as the specified fluxes, with the evaporative flux being computed using Fick's law. Water removal by transpiration of plants is treated as a sink term in Richards' equation (4). Transpiration is computed by applying the potential transpiration demand at each node within the root depth of the profile. Root length density at a particular depth is used to compute the actual transpiration fraction. Potential evapotranspiration (upper limit on actual evapotranspiration) is computed from the daily minimum and maximum air temperatures, net solar radiation, relative humidity, and daily wind speed using a modified form of Penman's equation as given by Doorenbos and Pruitt (1977). Soil-water storage is computed by integrating the water content profile. Flux from the lower boundary is percolation (Fig. 5).

### Geotechnical Input Data

Geotechnical data input to UNSAT-H consists of saturated hydraulic conductivities, porosities, and unsaturated hydraulic

properties of the cover soils. Input for the unsaturated hydraulic properties consists of fitting parameters for the soil-water characteristic functions and the unsaturated hydraulic conductivity functions. The input data are listed in Table 1.

### Vegetative Input Data

Vegetative input for UNSAT-H includes rooting depth, leaf area index (LAI), growing season, percent bare area (PBA), and parameters describing the root length density function (Fayer and Jones 1990). The vegetative input data are listed in Table 2. The growing season for vegetation in Richland, Wash., was used.

The LAI was recommended as 0.4 by the Soil Conservation Service's (SCS) office in Wenatchee, Wash., whose representatives visited the test section prior to making the recommendation. The rooting depth was assigned using measurements performed on specimens collected with sampling tubes. Field measurements of PBA were used as input. Benson et al. (1993) describe the methods used to measure rooting depth and PBA.

The root length density function used in UNSAT-H has the following form:

$$R = ae^{-bz} + b_2 \quad (5)$$

where  $R$  = normalized root length density;  $a$ ,  $b_1$ , and  $b_2$  = coefficients; and  $z$  = depth from surface of cover. Root length density functions for the vegetation were not measured. Instead, the root length density function for cheatgrass from Fayer and Jones (1990) was used. The vegetation on the test sections is similar to cheatgrass. Parameters for the root length density functions for both test sections are listed in Table 2.

### Meteorological Input Data

Meteorological input to UNSAT-H includes soil surface albedo, daily and hourly precipitation, daily maximum and minimum air temperatures, daily solar radiation, average daily dew point, and average daily wind speed. The albedo for the test sections was not measured, but Chudnovskii (1966) reports that an albedo of 0.1 is reasonable for wet soils and 0.3 is reasonable for dry soils. An average albedo of 0.2 was used. Otherwise, meteorological data collected on-site were used as input (Khire et al. 1994).

UNSAT-H does not have a snowmelt algorithm. Hence, precipitation in the form of snow has to be "melted" before it is input to UNSAT-H. To calculate daily snowmelt, the restricted degree-day radiation balance approach (Kustas et al. 1994) was used. In this method, daily snowmelt ( $M$ ) is computed using

$$M = a_r T_d + m_Q R_n \quad (6)$$

where  $a_r$  = restricted degree-day factor (ranging from 0.20 to 0.25  $^{\circ}\text{C}$ );  $T_d$  = average daily air temperature above base temperature (assumed  $0^{\circ}\text{C}$  in this study);  $m_Q$  = conversion constant equal to 0.026  $\text{W/m}^2$ ; and  $R_n$  = net solar radiation. An average albedo of 0.74 was used for the snow to calculate net solar radiation from the measured solar radiation. Kustas et al. (1994) and Benson et al. (1996) report that the average snow surface albedo is 0.85 for fresh dry snow, whereas it decreases

TABLE 2. Vegetative Information Input to UNSAT-H

Parameter (1)	Value (2)	Source (3)
Rooting depth (m)	0.15	Field-measured (Benson et al. 1993)
Percent bare area (%)	83	Field-measured (Benson et al. 1993)
Leaf area index	0.4	SCS recommendation
Growing season (Julian Day)	105–225	SCS recommendation
Fitting parameters for root density function	$a = 1.16$ , $b_1$ (1/m) = 12.9, $b_2 = 0.02$ (Cheatgrass)	Fayer and Jones (1990), Fayer and Walters (1995)

to 0.6 as the snow becomes saturated and contaminated near the end of the ablation (i.e., melting) period. Snowmelt computed using (6) was input to UNSAT-H as "rainfall" between 10 a.m. and 5 p.m., the times during which solar radiation was greatest. Snowmelt data were not collected, but periods during which snowmelt occurred were recorded.

Sublimation in semiarid regions can affect the quantity of snow that contacts the cover as water. Sublimation of snow was neglected, however, because it is difficult to predict and no sublimation data were available from the test section.

### Finite-Difference Nodal Arrangement and Control Criteria

A finite-difference grid consisting of 60 nodes was used to discretize the profile of the test section ( $D = 90$  cm in Fig. 5). A deeper profile was not considered, because the geomembrane provided a no-flow boundary at the bottom of the lysimeter. Soil and vegetative properties were assigned to each node. The nodal spacing was small (0.1 cm) near the boundaries and became progressively larger away from the boundaries (3 cm). These spacings are consistent with spacings recommended by Fayer and Jones (1990). Nodal spacing was selected to minimize mass balance errors while maintaining reasonable CPU times. Simulations described in this paper required about five days of computation time on a Hewlett-Packard 9000 C110 workstation equipped with 128 MB RAM.

A maximum time-step of 0.25/h and a minimum time-step of  $10^{-4}$ /h were used. The mass balance criterion was selected such that the error in water content of any node did not exceed  $10^{-4}$ . This mass balance criterion resulted in overall mass balance errors less than 0.5% ( $\sim 1$  mm precipitation). Mass conservation and equal suction are applied at the boundary between the layers.

### Initial and Boundary Conditions

Initial conditions for UNSAT-H were specified by assigning the initial head to each node in the finite-difference grid (Fig. 5). Matric suctions obtained from the soil-water characteristic curves (Fig. 3) corresponding to water contents measured in the field were used to determine initial heads.

The lower boundary can be specified as constant head, specified flux, or unit gradient, but the appropriate boundary for the base of the test section is not obvious. Matric suctions at the base change; thus a constant head boundary cannot be employed. The specified flux boundary is impossible, because percolation from the base is a desired unknown quantity that varies temporally. The unit downward gradient boundary condition is not necessarily correct, because flow can be upward or downward; but is reasonable if the bottom nodal spacing is very small. One of the conditions must be specified, and thus a unit downward gradient was selected because it is conservative, i.e., it always directs flow downward at the base of the test section, albeit usually at a very low rate. The bottom nodal spacing was 1 mm. A similar boundary condition was used by Fayer et al. (1992) when simulating the hydrology of final cover lysimeters constructed at the Hanford Site.

The upper boundary was specified as a variable flux boundary, which corresponds to evaporation or infiltration depending on the meteorological conditions. Fayer et al. (1992) also used the flux upper boundary condition.

### COMPARISON OF MODEL ESTIMATES WITH FIELD DATA

#### Surface Runoff

Measured surface runoff is shown in Fig. 6(a) with the precipitation record. The majority of runoff occurs in late fall,

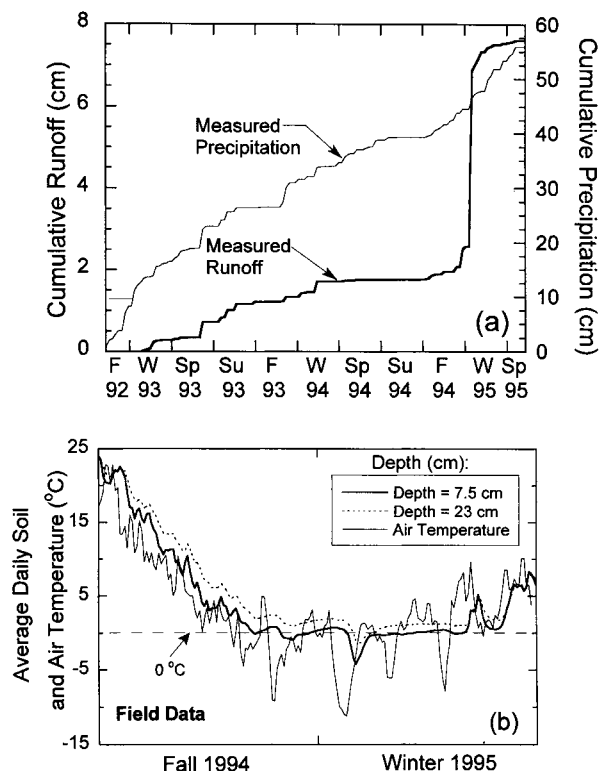


FIG. 6. Cumulative Runoff and Precipitation, and Average Daily Air and Soil Temperatures

winter, and spring, when most of the precipitation occurs. Runoff is generally a small fraction of the water balance ( $<10\%$ ). During late fall 1994 and early winter 1995, however, runoff was large because the ground surface was frozen [Fig. 6(b)], which limited infiltration (Khire et al. 1997). In addition, most of the precipitation during fall 1994 and winter 1995 was in the form of rain (7.4 cm)—little snowfall occurred (1.6 cm). Hence, only a small portion of precipitation could infiltrate; the remainder became runoff.

UNSAT-H estimated zero runoff for the capillary barrier for the entire monitoring period [Fig. 6(a)]. Most of the difference between measured and estimated runoff can be attributed to the frozen surface of the capillary barrier in fall 1994 and first half of winter 1995 [Fig. 6(b)]. Because UNSAT-H does not account for the impedance to infiltration by frozen ground, the model allowed snowmelt and rainfall to infiltrate during this period. UNSAT-H also estimated zero runoff in other seasons, but this error in the water balance is relatively small (2.7%) compared to errors incurred when the surface is frozen (Fig. 6). UNSAT-H probably underestimated runoff during these periods because it ignores hysteresis in the soil-water characteristic curve and the hydraulic conductivity function, and drying curves were used as input. For a given suction, lower unsaturated hydraulic conductivity exists during wetting than during drying, resulting in less infiltration.

Underestimating runoff generally results in a conservative estimate of percolation, because excess water is allowed to enter the soil profile (Khire et al. 1997). Better estimates of runoff, and thus more accurate estimates of percolation, can be made by predicting surficial temperatures of the cover and then adjusting the surface boundary conditions to reflect the frozen or unfrozen state of the cover surface. This type of procedure is used in the hydrologic evaluation of landfill performance (HELP) water balance model (Schroeder et al. 1994). However, accurately predicting surface temperature is difficult, and water balance errors incurred by inaccurate surface temperature predictions can be greater than those incurred

by ignoring the surface condition (Khire et al. 1997). Incorporating hysteresis into the model will also improve runoff estimates, but at additional computation expense. Alternatively, wetting curves could have been used, but wetting and scanning (wet-to-dry or dry-to-wet) curves are infrequently measured because of experimental difficulties. Thus, data to describe wetting or hysteresis may not be available.

### Soil-Water Content

Volumetric water contents measured at five depths (7.5 cm—silty layer; 23 cm, 38 cm, 53 cm, 69 cm—sand) are shown in Fig. 7(a). Increases in water content occur in fall and winter, followed by decreases in spring and summer. These changes in water content are consistent with the seasonal changes in precipitation and growing seasons in East Wenatchee.

During fall and winter, the silty layer gradually wets due to influx of precipitation. The capillary barrier effect, however, maintains low water contents in the underlying coarse-grained sand layer even while the finer-grained silty layer wets. However, once the water content in the silty layer approaches 0.3, water contents in the sand suddenly increase, almost simultaneously. For example, in winter 1993 [Fig. 7(b)], water contents in the sand do not increase until the water content of the silty layer reaches approximately 0.28.

As spring begins, water contents in both layers decrease [Fig. 7(b)] due to the start of the growing season and increased surface temperature, both of which yield greater evapotranspiration. In spring 1993, percolation also contributed to the reductions in water content in the sand layer. The water contents continue to decrease until they reach a minimum value, which is essentially the same each year. Thus, the hydrology of the cover each fall and winter is essentially independent of the hydrology in previous years, because the water contents at

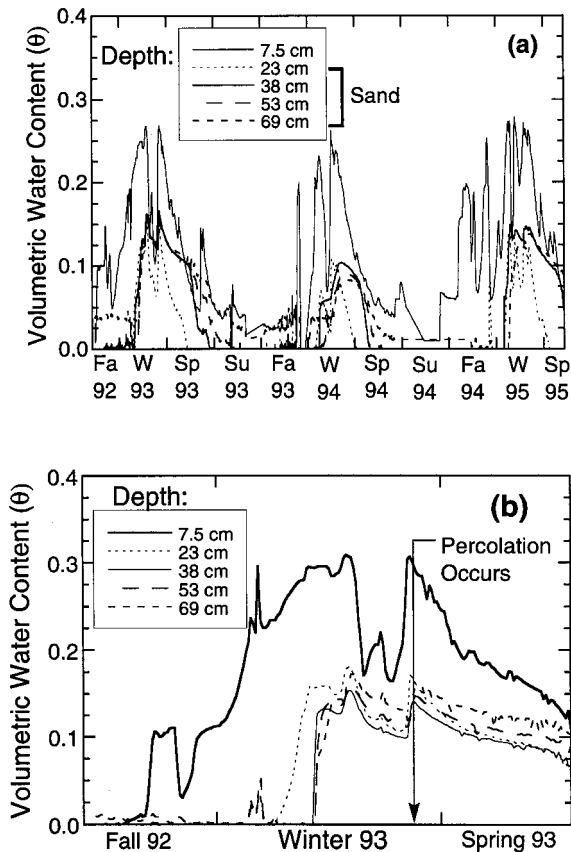


FIG. 7. Water Contents: (a) during Study Period; (b) during Fall 1992–Spring 1993

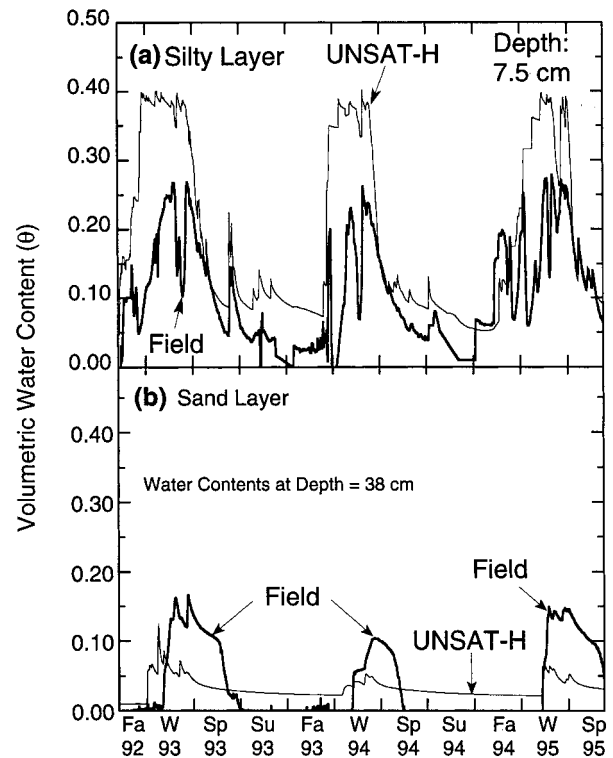


FIG. 8. Measured and Estimated Water Contents: (a) Silty Layer; (b) Sand at 38 cm

the onset of fall are essentially the same. This is true provided that physical changes (e.g., erosion gullies, vegetation changes, etc.) do not occur which affect performance of the barrier. A similar condition may not necessarily exist at other semiarid and arid sites, but it has also been observed in the prototype barrier at the Hanford site (Ward and Gee 1997; Gee et al. 1997). In some cases, water may reach depths from which it cannot be removed by evapotranspiration in spring and summer. In this situation, percolation through the barrier increases over time as water accumulates at depth (Morris and Stormont 1996).

Comparisons between measured and estimated water contents in the silty layer and mid-depth in the sand layer are shown in Fig. 8. Trends in the field data are reproduced by the model, but the model overestimates water contents in the silty layer and underestimates water contents in the sand. However, the model does capture the sudden jumps in water content caused by the capillary barrier effect. Water contents in the silty layer are overestimated because surface runoff is underestimated, which results in more water entering the soil. Water contents are underestimated in the sand because the geocomposite drain permits water to be stored in the sand that would otherwise drain in a deep sand layer or under unit gradient conditions. In addition, because the model ignores hysteresis, and drying curves for  $K_{\psi}$  were used, the hydraulic conductivity during wetting is overestimated, which permits water to drain more rapidly than would occur in the field.

### Soil-Water Storage

Measured and estimated soil-water storage are shown in Fig. 9. The field data show that soil-water storage increases in fall and winter and decreases during spring and summer, following the seasonal changes in water content [Fig. 7(a)]. UNSAT-H produced a similar trend. However, the annual peak soil-water storage was always underestimated, and in 1993 the increase and subsequent decrease in soil-water storage occurred too early.

Peak soil-water storage is underestimated for two reasons. First, the geocomposite drain in the test section allows the sand to store more water than the model permits using a unit gradient condition. Second, the model permits evapotranspiration to begin too early and thus evaporation is overestimated (Fig. 10).

The increase in soil-water storage from UNSAT-H occurs too early in 1993 because the snowmelt algorithm permitted snow to melt earlier than in the field. As a result, UNSAT-H suggested that a large increase in soil-water storage occurred five weeks earlier than in the field (Fig. 9). Similarly, UNSAT-H estimated a decrease in soil-water storage at the end of

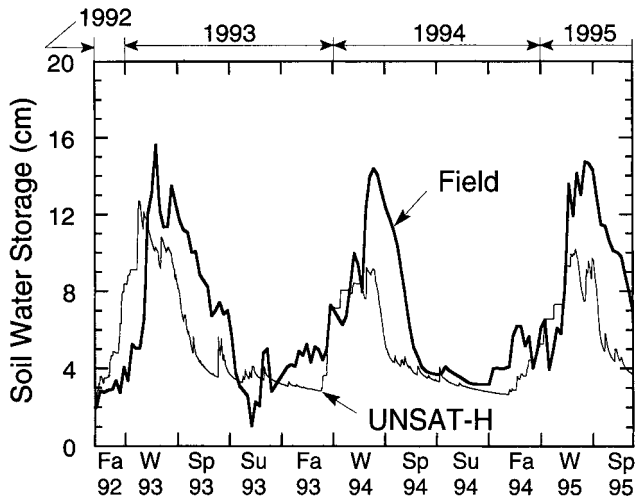


FIG. 9. Measured and Estimated Soil-Water Storage

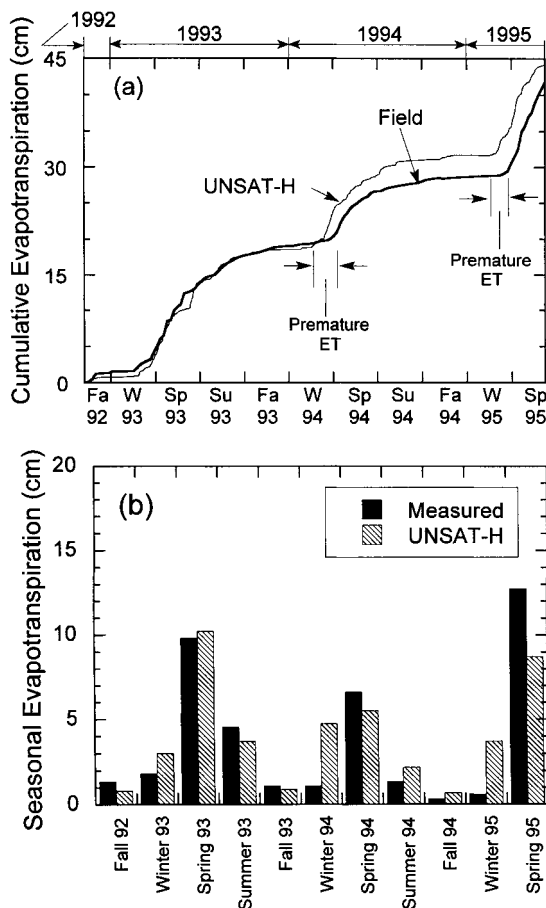


FIG. 10. Measured and Estimated Evapotranspiration: (a) Continuous Record; (b) Seasonal Averages

spring 1993 that was approximately five weeks earlier than the measured decrease in soil-water storage (Fig. 9). Field records show that most of the snowmelt occurred in mid-winter, whereas the snowmelt model (6) allowed the melt to occur in late fall. Simulations for both test sections conducted using a delayed snowmelt yielded a soil-water storage curve that matched fairly accurately with the field soil-water storage. The delay in snowmelt had no physical basis, however; it was selected to obtain a better match of the measured and estimated soil-water storage curves. In addition, simulations conducted where snow was applied immediately as rain (i.e., instantaneous melting) resulted in an even earlier increase in estimated soil-water storage (eight to nine weeks earlier than occurred in the field, Benson et al. 1993).

These results suggest that snowmelt predictions have a large impact on predictions of soil-water storage and the water balance of capillary barriers (see also subsequent section on percolation). Others have also observed the importance of snowmelt in the field. For example, rapid spring snowmelt of a thick snow pack caused significant percolation in field tests of capillary barriers conducted by Hakonson et al. (1994) in Utah. In addition, unexpected percolation occurred in unvegetated lysimeters at the Hanford site (Gee et al. 1993) and greater than expected soil-water storage occurred in the Hanford prototype barrier (Gee and Ward 1997) after melting of heavy snows in spring.

## Evapotranspiration

Measured and estimated evapotranspiration are shown in Fig. 10. The field data show that evapotranspiration occurs at the highest rate during spring and early summer, whereas it is at its lowest rate (essentially nil) during late summer, fall, and winter. These trends are consistent with well-established phenomena associated with changing seasons, available soil-water storage, and the beginning and ending of vegetative growth.

Evapotranspiration estimated by UNSAT-H is similar to that in the field through winter 1994. Beginning in late winter 1994, however, evapotranspiration was overestimated primarily because it began during winter, whereas evapotranspiration in the field was not significant until early spring. Most of the evapotranspiration estimated by UNSAT-H consisted of evaporation (80%). During late winter, snow cover and frozen surface conditions exist periodically, limiting evaporation from the soil (Khire et al. 1994). Had UNSAT-H accounted for these conditions and initiated evapotranspiration later, the estimated and measured annual evapotranspiration for 1994 and 1995 probably would have been closer. Similar overestimates in evapotranspiration have also been reported by Fayer et al. (1992).

## Percolation

Measured and estimated percolation are shown in Fig. 11. UNSAT-H overestimated percolation by 9 cm during the monitoring period. Most of the overestimation is in winter 1993 (6.5 cm), when heavy snowfall occurred and a thick snow pack formed. Smaller overestimates were obtained for winter and spring 1994 (1 cm) and winter and spring 1995 (1.5 cm). Percolation was overestimated for the following reasons: (1) The additional storage in the sand caused by the geocomposite drain is not considered by the model using the unit gradient boundary condition; (2) snowmelt was simulated prematurely; and (3) runoff was underestimated. Ignoring hysteresis in the soil hydraulic properties probably also contributed to the overestimation. The hydraulic conductivity curves for drying were used, and thus the hydraulic conductivity was probably overestimated. In addition, spatial variability of the cover soils, which was not considered in the modeling effort, may have



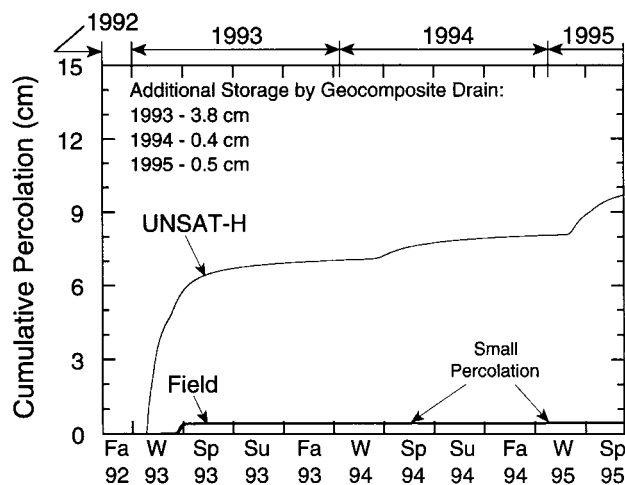


FIG. 11. Measured and Estimated Cumulative Percolation (Small Quantities of Percolation Were Measured in Spring 1994 and Winter 1995 and Are Noted as "Small Percolation")

contributed to the difference between measured and estimated percolation.

Additional percolation that would occur if the sand drained under a unit gradient boundary condition was estimated using the water content data. The additional percolation was 3.8 cm in spring 1993, 0.4 cm in spring 1994, and 0.5 cm in spring 1995. That is, the discrepancy in percolation can be attributed in part to storage in the sand layer that would not occur if the lower boundary was a unit gradient. Premature snowmelt and underestimation of runoff result also contributed by allowing too much water to enter the cover too early, particularly in winter 1993. Percolation from UNSAT-H began seven weeks earlier than occurred in the field, which is similar to the elapsed time between the simulated and actual snowmelt. Had the model simulated snowmelt later, more water would have been removed by evapotranspiration or stored within the cover, and less percolation would have been transmitted.

Percolation probably could be reduced from the capillary barrier by increasing the storage capacity of the surface layer, i.e., by increasing the surface layer thickness, improving the water-retention characteristics of the surface layer, or by improving water removal via better vegetation (Stormont and Morris 1998; Khire et al. 1998). In practice, the surface layer would be much thicker than that used in the test section. A thicker surface layer is needed to manage the water stored in the sand, which would percolate if an underlying coarse layer was not present, and to store water from extreme hydrologic events not encountered during the test period. More than adequate evapotranspiration potential exists at this site to extract water from a thicker layer storing more water, as evident by the near cessation of evapotranspiration by early to mid-summer (Fig. 10). Khire et al. (1998) discuss the importance of these variables in greater detail.

## CONCLUSIONS AND RECOMMENDATIONS

A comparison has been made between the measured water balance of a capillary barrier and the water balance estimated using the model UNSAT-H. Nearly all of the input required for UNSAT-H was measured in the field or laboratory. Trends from UNSAT-H were generally similar to trends observed in the field, with the exception of surface runoff, which was significantly underestimated. Evapotranspiration was overestimated in late winter and peak soil-water storage was underestimated. Water contents were estimated reasonably, although the changes in water content from UNSAT-H were not as large and occurred less quickly than in the field. Percolation was

generally overestimated, with the greatest overestimation occurring after a winter with substantial snowfall.

Most of the differences between measured and estimated quantities appear closely related to storage in the sand layer that was not accounted for using the unit gradient condition at the lower boundary, premature snowmelt, and underestimation of runoff. Had snowmelt and runoff been simulated more accurately, the model would have let less water into the cover at a later period, and this water would likely have been removed by evapotranspiration. In addition, the version of UNSAT-H that was used does not consider hysteresis in the soil hydraulic properties, which can result in the unsaturated hydraulic conductivity being too high during wetting events at a given suction if drying curves are used as input. Improving the model in these areas would improve its accuracy. Nevertheless, the comparison between measured and estimated water balance quantities is reasonably good given the complexity of hydrology in semiarid climates and unsaturated flow in capillary barriers. Thus, covers designed as capillary barriers using UNSAT-H and the snowmelt model by Kustas et al. (1993) are likely to transmit percolation similar to that predicted by the model. If very accurate predictions of percolation are required, however, field testing may be necessary.

This study has also shown that a capillary barrier performed in reasonable agreement with theory under natural meteorological conditions. That is, water was excluded from the coarse-grained layer until the overlying fine-grained layer was nearly saturated and the matric suction was low. Subsequently, water migrated into the coarse-grained layer. This study also shows that capillary barriers are prone to significant percolation when stressed by extreme hydrologic events, such as the large snow accumulation that occurred during winter 1993 in East Wenatchee. Snowmelt is a particularly challenging hydrological condition. Accordingly, the importance of extreme hydrological conditions should be considered when designing capillary barriers, to ensure that percolation emanating from the cover is not so large that ground-water contamination may occur.

## ACKNOWLEDGMENTS

The National Science Foundation (NSF) and WMX Technologies, Inc., provided financial support for this study. Support from NSF was provided through Grant No. CMS-9157116. The results and opinions expressed in this paper are those of the writers and are not necessarily consistent with policies or opinions of the sponsors. Thanks are expressed to Charles and Ty Pearsall of E. Wenatchee, Washington, and Xiaodong Wang of the University of Wisconsin-Madison, who assisted in construction, instrumentation, and maintenance of the test sections. The writers also express appreciation to Robert Pliska, who provided assistance throughout the study, and Glendon Gee, who provided thoughtful comments regarding alternative covers.

## APPENDIX. REFERENCES

- Allison, G., Gee, G., and Tyler, S. (1994). "Vadose-zone techniques for estimating groundwater recharge in arid and semiarid regions." *Soil Sci. Soc. of Am. J.*, 58, 6-14.
- Benson, C., Khire, M., and Bosscher, P. (1993). "Final cover hydrologic evaluation, phase II-final report." *Envir. Geotech. Rep. 93-4*, Dept. of Civil and Environmental Engineering, University of Wisconsin-Madison, Madison, Wisc.
- Benson, C., Bosscher, P., Lane, D., and Pliska, R. (1994). "Monitoring system for hydrologic evaluation of landfill final covers." *Geotech. Testing J.*, 17(2), 138-149.
- Benson, C., and Khire, M. (1995). "Earthen final covers for landfills in semi-arid and arid climates." *Landfill Closures, GSP No. 53*, R. Dunn and U. Singh, eds., ASCE, Reston, Va., 201-218.
- Benson, C., Olson, M., and Bergstrom, W. (1996). Temperatures of an insulated landfill liner, *Transp. Res. Rec.*, Transportation Research Board, Washington, D.C., No. 1534, 24-31.

- Benson, C., and Gribb, M. (1997). "Measuring unsaturated hydraulic conductivity in the laboratory and field." *Unsaturated Soil Engineering Practice*, GSP No. 68, S. Houston and D. Fredlund, eds., ASCE, Reston, Va., 113–168.
- Benson, C., and Wang, X. (1998). "Soil water characteristic curves for solid waste." *Envir. Geotech. Rep. 98-13*, Dept. of Civil and Environmental Engineering, University of Wisconsin–Madison, Madison, Wisc.
- Benson, C., Albrecht, B., Motan, E., and Querio, A. (1998). "Equivalency assessment for an alternative final cover proposed for the Greater Waukegan Regional Landfill and Recycling Center." *Envir. Geotech. Rep. 98-6*, Dept. of Civil and Environmental Engineering, University of Wisconsin–Madison, Madison, Wisc.
- Chudnovskii, A. (1966). "Plants and light. I. Radiant energy." *Fundamentals of Agrophysics*, Israel Program for Scientific Translations, Jerusalem, 1–51.
- Doorenbos, J., and Pruitt, W. (1977). "Guidelines for predicting crop water requirements." *FAO Irrigation Paper No. 24*, 2nd Ed., Food and Agricultural Organization of the United Nations, Rome, 1–107.
- Dwyer, S. (1997). "Cost comparisons of alternative landfill final covers." *Proc., Int. Contain. Tech. Conf.*, U.S. Dept. of Energy, Germantown, Md., 400–406.
- Fayer, M., and Jones, T. (1990). *Unsaturated soil-water and heat flow model, ver. 2.0*. Pacific Northwest Laboratory, Richland, Wash.
- Fayer, M., Rockhold, M., and Campbell, M. (1992). "Hydrologic modeling of protective barriers: Comparison of field data and simulation results." *Soil Sci. Soc. of Am. J.*, 56, 690–700.
- Fayer, M., Gee, G., Rockhold, M., Freshley, M., and Walters, T. (1996). "Estimating recharge rates for a groundwater model using a GIS." *J. Envir. Quality*, 25, 510–518.
- Fleenor, W., and King, I. (1995). "Identifying limitations on use of the HELP model." *Landfill Closures*, GSP No. 53, R. Dunn and U. Singh, eds., ASCE, Reston, Va., 121–138.
- Gee, G., and Hillel, D. (1988). "Groundwater recharge in arid regions: Review and critique of estimation methods." *J. of Hydrol. Processes*, 2, 255–266.
- Gee, G., Fayer, M., Rockhold, M., and Campbell, M. (1992). "Variations in recharge at the Hanford site." *Northwest Sci.*, 66, 237–250.
- Gee, G. et al. (1993). *Field Lysimeter Test Facility Status Rep. IV: FY 1993*, Pacific Northwest Laboratory, Richland, Wash.
- Gee, G., Wierenga, P., Andraski, B., Young, M., Fayer, M., and Rockhold, M. (1994). "Variations in water balance and recharge potential at three western sites." *Soil Sci. Soc. of Am. J.*, 58, 63–72.
- Gee, G., Ward, A., and Fayer, M. (1997). "Surface barrier research at the Hanford site." *Proc., Intl. Contain. Tech. Conf.*, U.S. Dept. of Energy, Germantown, Md., 305–311.
- Gee, G., and Ward, A. (1997). "Still in quest of the perfect cap." *Proc., Landfill Capping in the Semi-Arid West: Problems, Perspectives, and Solutions*, Envir. Sci. and Res. Found., Idaho Falls, Idaho, 145–164.
- Hakanson, T., Lane, L., and Springer, E. (1992). "Biotic and abiotic processes." *Deserts as Dumps, the Disposal of Hazardous Materials in Arid Ecosystems*, C. Reith and B. Thomson, eds., University of New Mexico Press, Albuquerque, N.M.
- Hakanson, T. et al. (1994). "Hydrologic evaluation of four landfill cover designs at Hill Air Force Base, Utah." *LAUR-93-4469*, Dept. of Energy Mixed Waste Landfill Integrated Demonstration, Sandia National Laboratory, Los Alamos, N.M.
- Haverkamp, R., Valcin, M., Touma, J., Wierenga, P., and Vauchaud, G. (1977). "A comparison of numerical simulation models for one-dimensional infiltration." *Soil Sci. Soc. of Am. J.*, 41, 285–294.
- Hillel, D. (1980). *Fundamentals of Soil Physics*. Academic Press, San Diego.
- Khire, M., Benson, C., and Bosscher, P. (1994). "Final cover hydrologic evaluation—phase III." *Envir. Geotech. Rep. 94-4*, Dept. of Civil and Environmental Engineering, University of Wisconsin–Madison, Madison, Wisc.
- Khire, M. (1995). "Field hydrology and water balance modeling of earthen final covers for waste containment," PhD dissertation, University of Wisconsin–Madison, Madison, Wisc.
- Khire, M., Benson, C., and Bosscher, P. (1997). "Water balance modeling of earthen final covers at humid and semi-arid sites." *J. of Geotech. and Geoenviron. Engrg.*, ASCE, 123(8), 744–754.
- Khire, M., Benson, C., and Bosscher, P. (1998). "Capillary barriers in semi-arid and arid climates: Design variables and the water balance." *Envir. Geotechnics Rep. 98-14*, Dept. of Civ. and Envir. Engrg., University of Wisconsin, Madison, Wis.
- Kustas, W., Rango, A., and Uijlenhoet, R. (1994). "A simple energy budget algorithm for the snowmelt runoff model." *Water Resources Research*, 30(5), 1515–1527.
- Landeen, D. (1994). "The influence of small-mammal burrowing activity on water storage at the Hanford site." *In Situ Remediation: Scientific Basis for Current and Future Technologies*, G. Gee and N. Wing, eds., Battelle, Columbus, Ohio, 523–543.
- Link, S., Wing, N., and Gee, G. (1995). "The development of permanent isolation barriers for buried wastes in cool deserts: Hanford, Washington." *J. of Arid Land Studies*, 4, 215–224.
- Litgotke, D. (1994). "Control of eolian soil erosion from waste site surface barriers." *In Situ Remediation: Scientific Basis for Current and Future Technologies*, G. Gee and N. Wing, eds., Battelle, Columbus, Ohio, 545–559.
- Meerdink, J., Benson, C., and Khire, M. (1996). "Unsaturated hydraulic conductivity of two compacted barrier soils." *J. of Geotech. Engrg.*, ASCE, 122(7), 565–576.
- Meyer, P., Rockhold, M., Nichols, W., and Gee, G. (1996). *Hydrologic evaluation methodology for estimating water movement through the unsaturated zone at commercial low-level radioactive waste disposal sites*. Pacific Northwest Laboratory, Richland, Wash.
- Morris, C., and Stormont, J. (1996). "Design of capillary barriers for waste site containment." *Proc., 3rd Int. Sym. on Envir. Geotechnol.*, H-Y Fang and H. Inyang, eds., Technomic, Lancaster, Pa., 1, 513–522.
- Morris, C., and Stormont, J. (1997). "Capillary barriers and subtitle D covers: Estimating equivalency." *J. Envir. Engrg.*, ASCE, 123(1), 3–10.
- Mualem, Y. (1976). "A new model for predicting the hydraulic conductivity of unsaturated porous media." *Water Resour. Res.*, 12, 513–522.
- Nativ, R. (1991). "Radioactive waste isolation in arid zones." *J. Arid Envir.*, 20, 129–140.
- Nichols, W. (1991). *Comparative simulations of a two-layer landfill barrier using the HELP v. 2.0 and UNSAT-H v. 2.0 codes*. Pacific Northwest Laboratory, Richland, Wash.
- Nyhan, J., Hakanson, T., and Drennon, B. (1990). "A water balance study of two landfill cover designs for semiarid regions." *J. Envir. Quality*, 19, 281–288.
- Nyhan, J., Schofield, T., and Starmer, R. (1997). "A water balance study of four landfill cover designs varying in slope for semiarid regions." *J. of Envir. Quality*, 26, 1385–1392.
- Nyhan, J., Langhorst, G., Martin, C., Martinez, J., and Schofield, T. (1993). "Hydrologic studies of multilayered landfill closure of waste landfills at Los Alamos." *Proc., 1993 DOE Envir. Remediation Conf.*, Department of Energy, Washington, D.C.
- Schroeder, P., Lloyd, C., and Zappi, P. (1994). *The hydrologic evaluation of landfill performance (HELP) model, user's guide for version 3.0*. USEPA, Cincinnati, Ohio.
- Stormont, J., and Anderson, C. (1998). "Capillary barrier effect from an underlying coarser layer." *J. Geotech. and Geoenviron. Engrg.*, ASCE, in press.
- Stormont, J. (1995). "The performance of two capillary barriers during constant infiltration." *Landfill Closures*, GSP No. 53, J. Dunn and U. Singh, eds., ASCE, Reston, Va., 77–92.
- Stormont, J., and Morris, C. (1997). "Unsaturated drainage layers for diversion of infiltrating water." *J. Irrig. and Drain. Engrg.*, ASCE, 123(5), 364–366.
- Stormont, J., and Morris, C. (1998). "Method to estimate water storage capacity of capillary barriers." *J. of Geotech. and Geoenviron. Engrg.*, ASCE, 124(4), 297–302.
- Tanner, C. (1967). "Measurement of evapotranspiration." *Irrigation of Agricultural Lands*, American Society of Agronomy, Madison, Wisc., 534–574.
- van Genuchten, M. (1980). "A closed-form equation for predicting the hydraulic conductivity of unsaturated soils." *Soil Sci. Soc. Am. J.*, 44, 892–898.
- Ward, A., and Gee, G. (1997). "Performance evaluation of a field-scale surface barrier." *J. Envir. Quality*, 26, 694–705.